INTERNATIONAL ATOMIC ENERGY AGENCY

NUCLEAR DATA SERVICES

DOCUMENTATION SERIES OF THE IAEA NUCLEAR DATA SECTION

IAEA-NDS-201
March 1997

NRABASE 2.0

Charged-particle nuclear reaction data for Ion Beam Analysis

by

A.F. Gurbich
Obninsk, Russia

Abstract: For 30 targets between H-1 and Ag-109, differential cross sections for reactions induced by protons, deuterons, He-3 and alpha particles are given in tabular and graphical form. The data were compiled from original experimental references. The database was developed under a research contract with the IAEA Physics Section and is available on diskette from the IAEA Nuclear Data Section.

Nuclear Data Section
International Atomic Energy Agency
P.O. Box 100
A-1400 Vienna
Austria

e-mail, INTERNET: SERVICES@IAEAND.IAEA.OR.AT
fax: (43-1)20607
cable: INATOM VIENNA a
telex: 1-12645 atom a
telephone: (43-1)2060-21710

online: TELNET or FTP: IAEAND.IAEA.OR.AT
username: IAEANDS for interactive Nuclear Data Information System
username: ANONYMOUS for FTP file transfer
username: FENDL for FTP file transfer of FENDL files
For users with web-browsers: http://www-nds.iaea.or.at

Note:

The IAEA-NDS-reports should not be considered as formal publications. When a nuclear data library is sent out by the IAEA Nuclear Data Section, it will be accompanied by an IAEA-NDS-report which should give the data user all necessary documentation on contents, format and origin of the data library.

IAEA-NDS-reports are updated whenever there is additional information of relevance to the users of the data library.

For citations care should be taken that credit is given to the author of the data library and/or to the data center which issued the data library. The editor of the IAEA-NDS-report is usually not the author of the data library.

Neither the originator of the data libraries nor the IAEA assume any liability for their correctness or for any damages resulting from their use.

96/11

Citation guideline:

This database should be cited as follows:

> A.F. Gurbich, NRABASE 2.0, Charged-particle nuclear reaction data for Ion Beam Analysis; documented in the IAEA report IAEA-NDS-201 (1997). PC diskette received from the IAEA Nuclear Data Section.

NRABASE 2.0

Charged-particle nuclear reaction data for Ion Beam Analysis

Alexander F. Gurbich
Institute of Physics and Power Engineering
Obninsk, Russia

This database contains differential cross sections for reactions induced by protons, deuterons, He-3 and alpha particles on H-1, H-2, He-3, Li-6, Li-7, Be-9, B-10, B-11, C-12, C-13, N-14, N-15, O-16, O-18, F-19, Na-23, Mg-nat, Al-27, Si-28, P-31, S-32, Cl-nat, Ti-48, Cr-52, Fe-56, Se-nat, Br-nat, Zn-nat, and Ag-109. Tabulated experimental data as well as graphs can be displayed on the PC screen. In addition, comments and the related bibliographical references can be displayed or printed. The database was developed under a research contract (#8883) with the IAEA Physics Section.

The diskette contains 5 files including the self-extracting archive file NRA.EXE. The hardware requirements are: IBM PC or compatible with EGA or VGA monitor, about 3 MB free disk space.

In the following pages, the author's description of NRABASE 2.0 and the work achieved under the IAEA research contract is reproduced: "Compilation, measurements and evaluation of nuclear cross sections for use in ion beam analysis" (A.F. Gurbich).

1. Introduction.

The ion beam analysis (IBA) methods except for RBS strongly rely on the available experimental cross section data. These cross section data are especially important while planning an experiment and for computer simulation of measured spectra. There are several nuclear cross section databases but they provide data mainly for nuclear physics and some technical applications others than IBA. It became clear in the workshops held on this subject in Namur [1] and during the 12th and 13th IBA conferences that the needs of the IBA community and that of the nuclear science and engineering are different. The goal of this contract is to identify, collect, evaluate, and measure cross section data vital to the IBA community.

Many nuclear reaction cross sections were measured in the fifties and sixties by nuclear physicists. Most of these data are available from the literature but mainly as graphs. Besides, there are several problems with these data from the point of view of IBA. The main goal of these cross section measurements was to prove nuclear models and deduce adjustable parameters for those models. Therefore, the nuclear reactions that were studied were chosen based on the usefulness of the reaction for that particular theoretical model (e.g. even-even or odd-odd nuclei, etc.) In case of IBA those cross sections are needed that involve the nuclei whose concentration or depth profile should be determined in a given sample. The energy interval and angles at which measurements were performed are often out of range normally used in IBA. Therefore, although a large amount of cross section data seems to be available, most of it is unsuitable for IBA. An attempt to prepare a detailed inventory of all reactions of interest or potential interest to IBA has been made in Schonland Research Centre for Nuclear Sciences, South Africa [2].

Because of lack of required data most research groups doing IBA analytical work started to measure cross sections for their own use every time when an appropriate cross section was not found. As a result, papers with tabulated cross sections are not scarce now. However, these data should be evaluated prior to their widespread use. As far as differential cross section rather than total ones are used usually in IBA these data can be immediately employed only in the case of a scattering geometry very close to the reported one. Due to historical reasons charged particles detectors are mounted in the scattering chambers used in different laboratories at different fixed angles in the interval approximately from 130° to 180°. Meanwhile, cross section may strong depend on scattering angle in some cases. Theoretical model description of available data followed by extrapolation over angles of interest is needed to overcome this problem. Besides, it should be noted that the errors of cross section absolutization cancel for IBA analytical work made using the same setup that was employed while cross section measurements but they can cause an essential inaccuracy being used by another group. The IBA groups often apply thick target measurements in order to determine absolute cross section against internal standard for

which Rutherford scattering is assumed. This method needs none of the quantities usually defined with significant inaccuracy such as particles fluence or detection geometry but in this case errors are introduced by use of stopping power data. Hence in both cases a comparison of the results obtained by different groups should be done in order to produce reliable recommended cross section data. A *vice versa* process to that made when nuclear models were developed should now be applied to evaluate measured cross sections on the base of their consistency with nuclear models.

Low energy nuclear physics is regarded nowadays as a sufficiently studied field. Reaction mechanisms are known and appropriate models have been developed. However, satisfactory agreement between measured data and theoretical calculations which is sufficient as a rule in order to support a model does not provide reliable base for cross section *a priory* prediction. In addition nuclear reaction models use many adjustable parameters. Though some systematics and "global" sets of these parameters exist, fitting is always needed in order to represent a particular cross section. Moreover, in some important for IBA cases reaction mechanisms are in general known but there is no code which provide necessary calculations (see section 3.3). The problem for IBA community is also lack of expertise in nuclear physics which is needed to apply its methods.

In spite of the fact that the problem of cross section data for IBA is positively recognized by IBA community the work in this direction is not actually organized. As a result of the discussions mentioned above an electronic database (Sigmabase) was developed on trial basis at the Institute of Geological and Nuclear Sciences, New Zealand (I.C.Vickridge) and at the Idaho State University, USA (G.Vizkelethy). But this database contains only few required information presented as raw measured data and it is not actually maintained since it was established about three years ago.

It is evident that the problem can be resolved only as a result of significant coordinated efforts comparable with that in nuclear science and engineering where many years experience results in establishing a firm base for required nuclear data.

2. Development of NRABASE.

The first version of the NRABASE was developed in the end of 1994. That version is available from Sigmabase via Internet till now. The development of the NRABASE was made by incorporation of new data and by improvement of its structure and data presentation. The current status of the NRABASE content is shown in Table 1. The previous version of the NRABASE can be taken via Internet for comparison. It is available from the SigBase FTP Archive at *lhn.gns.cr.nz* or from its mirror at *physics.isu.edu*.

Table 1.

Current content of the NRABASE. Figures stand for number of data files.

	p,p$_0$	p,α_0	p,γ	p,$\alpha\gamma$	p,p'γ	d,d$_0$	d,p$_0$	d,p'	d,α_0	d,α'	^{3}He,p$_0$	^{3}He,p'	^{3}He,α_0	α,α_0	α,p$_0$
^{1}H															11
^{2}H											1			3	
^{3}He							2								
^{6}Li	5	3													
^{7}Li	8	10													
^{9}Be	1								1						
^{10}B	1	1							1	1					
^{11}B	1	1													
^{12}C	9		2			2	5				3	6	1	9	
^{13}C							1		1						
^{14}N	7					1	2	5	3	3		10	2	6	1
^{15}N		6		1					1						
^{16}O	7		2			2	4	7	6					10	
^{18}O	1	11													
^{19}F	6	4													
^{23}Na	1		2	2	2		1		1						
^{nat}Mg	1														
^{27}Al	3		2	1	2										
^{28}Si	3														
^{31}P			1	1	1										
^{32}S	2														
^{nat}Cl	1														
^{48}Ti	1														
^{52}Cr			1												
^{nat}Cr	1														
^{56}Fe	1														
^{nat}Se	1														
^{nat}Br	1														
^{nat}Zn	1														
^{109}Ag	1														

Graphs were stored using HP Graphic Language in the first version of the NRABASE. An additional possibility to display PCX formatted images has been developed. Graphs obtained with scanner may be immediately placed now into corresponding subdirectory. Data alignment at decimal point was introduced in the "Data" window. Scroll bars, which show the relative portion of the information visible in the window are added in the "Data" and "Comments" windows. Some technical improvements have also been made.

A great amount of information published only in a graphical form was digitized in the first version of the NRABASE using optical instruments. A new procedure described below has been developed in the course of the project implementation.

The appropriately enlarged graph image obtained with scanner and stored in the PCX format is displayed onto a PC screen. A special program is then used to transform the coordinates of a marker position into cross section and energy values. Some points belonging to x- and y-axes are first marked and the corresponding values of energy and cross section are entered to define the scales. Experimental points drawn in the graph are then marked. In order to take account of inevitable slope of the graph image against the screen sides the axes directions are parameterized using a mean least squares method and marked points coordinates x and y are then transformed according to

$$x' = x \cdot \cos\varphi + y \cdot \sin\varphi$$
$$y' = -x \cdot \sin\varphi + y \cdot \cos\varphi$$

where φ - is the axes tilt angle. Actual values of energy and cross section are finally obtained using the scale factors. Since the image size may exceed that of the screen (640x480 of pixels for VGA screen) the image can be scrolled in both x and y directions displaying a 640x480 fragment, all the marked points being moved with the image. The digitizing procedure was verified using some data available both as graph and table. Typical results obtained for data from Ref.[3] are shown in Table 2.

To obtain the worst possible conditions the image was deliberately tilted to the scanning direction by about 10°. It was proved by performed tests that both shift of scale and random deviations of points do not exceed in general some tenth of per cent. However, some points drop out up to ~2.5 per cent. It is seen that all these figures are well within experimental errors usually reported. It should be mentioned that the obtained results include the accuracy of the original drawing and the distortions introduced by a publisher. It is worth noting for comparison that for the procedure used to digitize the cross section plots in recently published Handbook [4] the lower limit of the uncertainty was reported to be 5%.

The second version of the NRABASE is attached to the present report as a selfextracting archive file saved on a diskette. Some additional information concerning the NRABASE was published in Ref.[5] which is also attached to the report. Note that the content of the NRABASE presented in the Table 1 is essentially updated as compared with corresponding table in Ref.[5]. Since the work with NRABASE is in progress some of the data shown are presented only by a graph or a table or even only by a reference. The block-diagram of the NRABASE is also presented in Ref.[5].

Table 2.
Results of digitizing procedure test.

Energy (MeV)			Cross section (σ/σ_R)		
Digitized	Original	Rel.error (%)	Digitized	Original	Rel.error (%)
1.005	1.000	- 0.487804	1.427	1.43	0.209790
1.020	1.025	0.499999	1.410	1.41	0
1.045	1.050	0.476190	1.376	1.38	0.289855
1.069	1.075	0.558139	1.364	1.34	-1.79104
1.096	1.100	0.363636	1.386	1.39	0.287769
1.121	1.125	0.355555	1.413	1.44	1.875000
1.146	1.150	0.347826	1.424	1.42	-0.28169
1.171	1.175	0.340425	1.417	1.45	2.275862
1.196	1.200	0.333333	1.411	1.42	0.633802
1.222	1.225	0.244897	1.405	1.40	-0.35714
1.248	1.250	0.160000	1.427	1.43	0.209790
1.273	1.275	0.568620	1.437	1.47	2.244897
1.298	1.300	0.538460	1.397	1.40	0.214285
Mean error value: 0.267578			Mean error value: 0.44701		
Errors standard deviation: 0.253580			Errors standard deviation: 1.08324		

3. Development of theoretical model evaluation.

3.1. Non-Rutherford elastic scattering.

There is a number of benefits in use of elastic scattering technique at "higher-than-usual" energies. First of all at higher energies light ions elastic scattering cross section for light elements rapidly increases whereas it still follows $1/E^2$ energy dependence for heavy nuclei. Thus high sensitivity for determination of light contaminants in heavy matrix is achieved. Besides, a depth of sample examination is enhanced. Over past few years non-Rutherford backscattering has been acknowledged to be a very useful tool in material analysis. Cross section measurements were reported for carbon, nitrogen, oxygen, sodium, aluminum, and many others nuclei (see Table 1). It should be noted that not only light elements cross section is needed for backscattering analysis but also knowledge of energy at which heavy matrix scattering is no longer pure RBS is important. In a series of works by Bozoian and Bozoian et al. [6-] a classical model has been developed to predict a threshold of cross section deviation from Rutherford formulae. From the nuclear physics point of view it is evident that this model treats the projectile-nucleus interaction in quite irrelevant way which should not provide realistic results. It often agrees with experimental data solely because of the fact that Coulomb barrier height is involved in the model. On the other hand, contrary to the authors opinion this model definitely disagree with experiment that was clearly shown in Ref.[7]. Hence, as far as an appropriate physics is not involved one

cannot rely upon the results obtained using this model in a particular case. The fact however is that this model is often used due to lack of alternative. More realistic results grounded on optical model calculations have been published recently by Bozoian in the Handbook of Modern Ion Beam Materials Analysis [4, p.509]. Unfortunately the utility of these data is doubtful since a scattering angle for which the results have been obtained is not known. Nor is quoted optical model parameters set which was used in the calculations. It is known that the results of calculations strongly depend on both of these input data.

Due to more than 30 years of application of the optical model the general features of phenomenological optical potential parameters are well established. An intensive study of the low energy anomalies in the optical potential behavior was made in early 80s. The peculiarities which were found are as follows. Strength parameters often have strong energy dependence in the vicinity of the Coulomb barrier, real potential radial dependence is of more complicated than Saxon-Woods form, imagine part of potential reveals non-systematic dependence on nucleus mass number, absorption is peaked at the nucleus surface, radius of the imagine potential diminishes with decreasing energy while its diffuseness increases. Calculations in framework of the optical model are very sensitive to the parameters used. So results obtained with global sets such as [8,9] appear to be unrealistic. Several attempts have been made to develop a global set for low energy region (see e.g.[10]) but reliable results may be expected only in case of calculations with parameters fitted to the experimental data. Thus only inter- or extrapolation over narrow angle or energy intervals is expected to be reliable. A detailed discussion of the low energy optical potential behavior and related physics may be found elsewhere [11].

Calculations in the present work were performed using SCAT2 code [12]. Some modification of the code have been made. In order to take into account a surface peaked term in the real part of the potential which originate from a dispersive relation [13] a derivative of the Saxon-Woods formfactor was added to the real potential. A modified optical potential has a real central part which is given in usual notation by

$$V_R(r) = -V_R f(r,r_R,a_R) + 4V_S a_S \frac{d}{dr} f(r,r_S,a_S),$$

where $f(r,r_X,a_X) = [1+exp(r-r_X A^{1/3})/a_X]^{-1}$ and V_S is the depth of the surface dip. Optimizing fitting procedure based on gradient method was developed which uses the SCAT2 as subroutine. As a result both angular distributions and excitation functions can be used to adjust the model parameters. An example of model approach to data evaluation is presented below.

Tabulated with a 100 keV step proton elastic scattering cross section data for ^{16}O at $\vartheta_{lab}=170°$ in the energy range from 2800 to 3100 keV from Ref.[14] were used to adjust optical

model parameters. The point at 2700 keV was omitted since it is too close to the resonance at 2663 keV.

The following set of the parameters has been found: V_R=55.36-1.1E MeV, r_R=1.23 fm, a_R=0.65 fm, W_D=0.472 MeV, r_D=1.30 fm, a_D=0.65 fm, $V_{s.o.}$=5.0 MeV, $r_{s.o.}$=1.01 fm, $a_{s.o.}$=0.65 fm, r_C=1.23 fm. The optimal parameters appear to be in a reasonable agreement with Ref.[15] where theoretical fit to the $^{16}O(p,p)^{16}O$ differential scattering cross section measured at 171.5° c.m. in the energy range from 400 to 1900 was made. A stronger energy dependence of the central real part of the potential

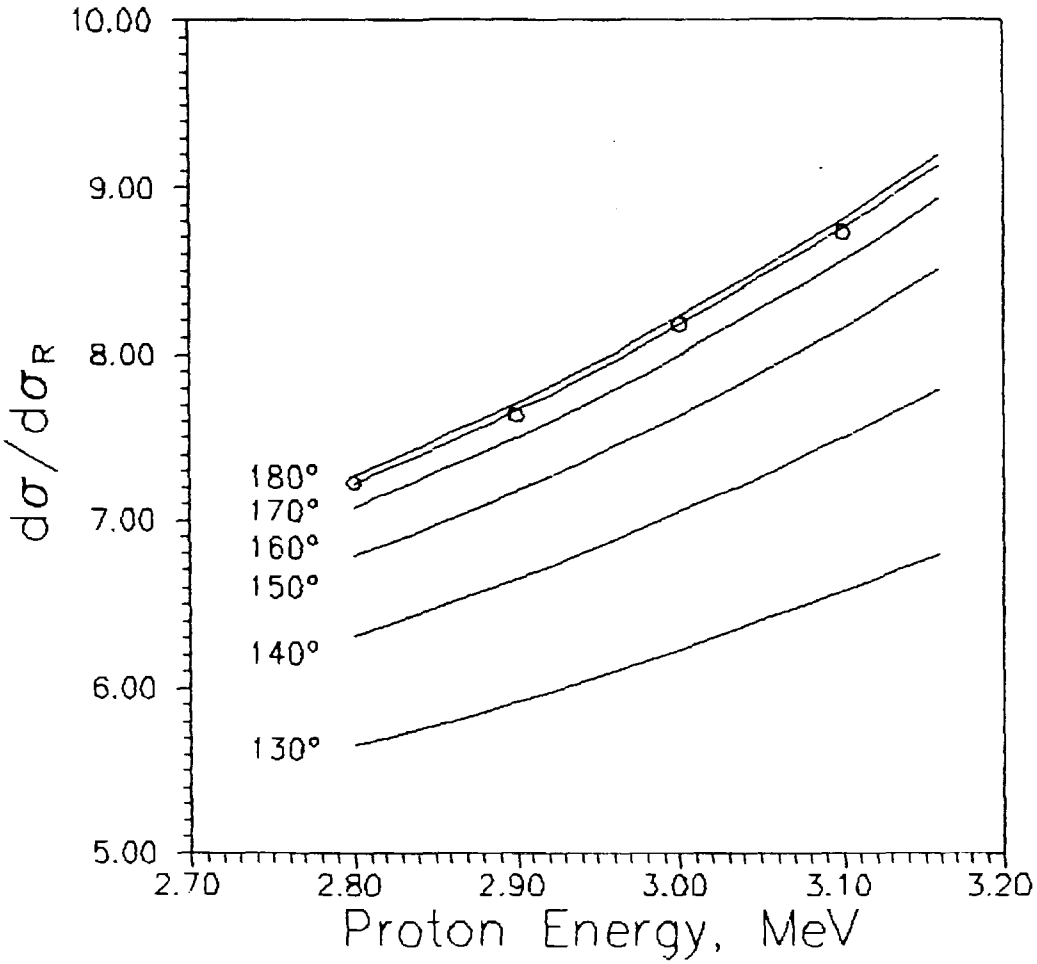

Fig.1. Theoretical evaluation of the $^{16}O(p,p)^{16}O$ cross section (curves) and experimental data used while optical model parameters fit (circles).

found in the present work is often observed in low energy region (see [11]). Nonzero W_D value is due to (p,γ)-channel contribution to the absorption which increases with increasing energy. The

cross sections for angle interval from 130° to 180° calculated using optimal optical model parameters are presented in Fig.1. along with experimental data from Ref.[14].

The consistency of the theoretical results with proton angular distribution measured in work [16] at 2382 keV is demonstrated in Fig.2. The authors of Ref.[16] have made an attempt to represent their data by optical model calculations. The calculations were made with arbitrary parameter set and as a result a conclusion was drawn that theoretical results did not represent the data. A polynomial fit shown in Fig.2 by dashed line was used by the authors of Ref.[16] instead

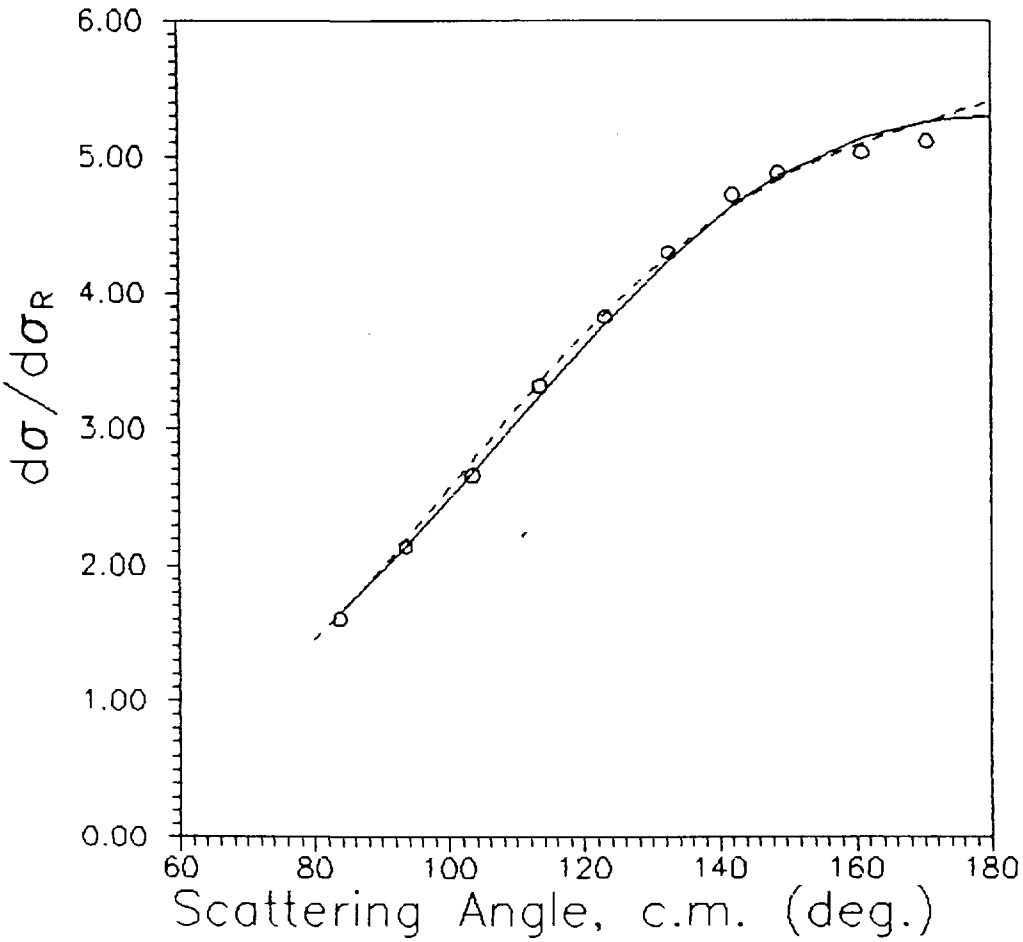

Fig.2. Experimental angular distribution of elastically scattered protons for $^{16}O(p,p)^{16}O$ scattering taken from Ref.[16] (circles) and optical model prediction (solid line). Polynomial fit to the data from Ref.[16] is shown by dashed line.

of a theory to evaluate the cross section. It is evident that in the range of interest (130° - 180°) a distinguishable difference between theory and fit is observed only near 180° where none of experimental points exists. This difference is about 2.3%. It is worth noting that a cross section in

close vicinity of 180° is important in case when annular detector is used. Taken into account that theoretical prediction which is based on the data from another work appears to be in very close agreement with experimental data of Ref.[16] the conclusion may be drawn that the theoretical results are grounded on the true physics of the process.

Extrapolation of the optical model results on the energy region below 2.0 MeV (Fig.3) demonstrate a fair agreement with available experimental data [15]. Thus obtained by fit to 4 experimental points model appears to be valid to represent cross sections over a sufficiently wide energy interval. Bozoian model prediction [6] of the proton energy at which the scattering cross section deviates by 4% from its Rutherford value is shown in the Fig.3 by dashed lines. It is evident that this prediction is unrealistic.

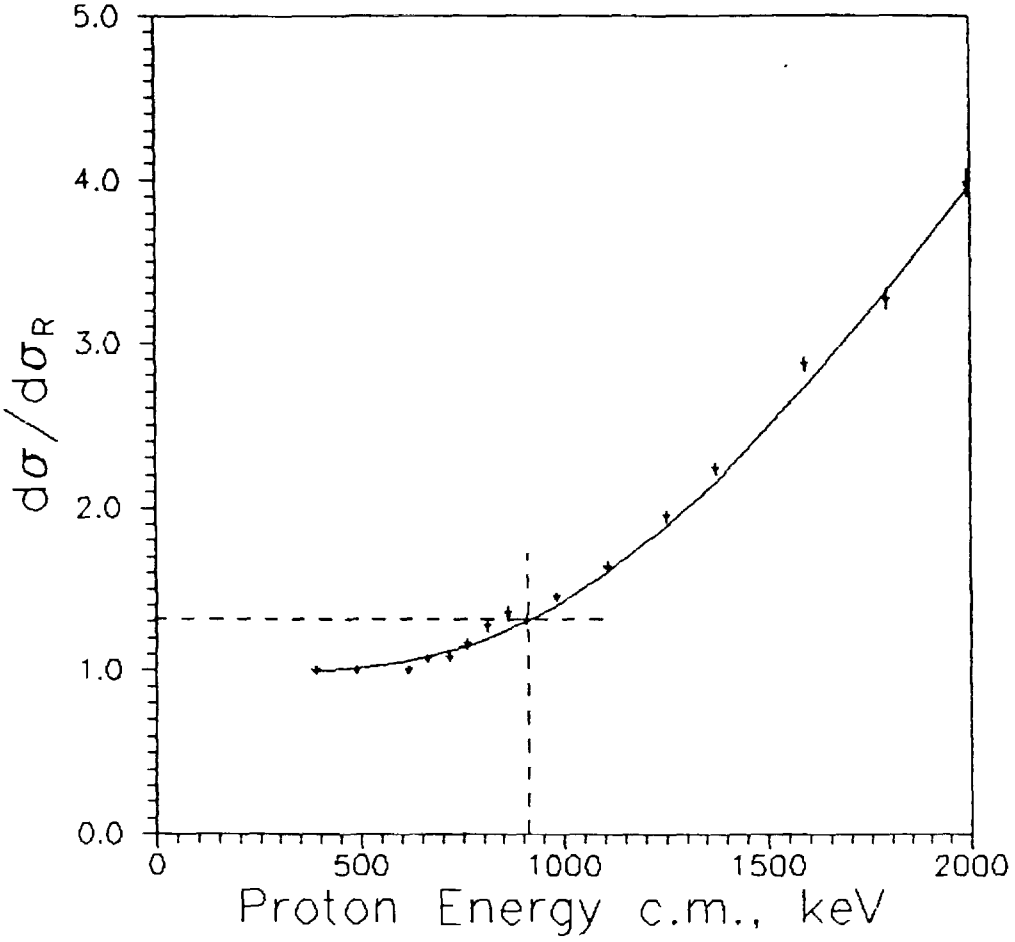

Fig.3. Comparison of the optical model prediction of proton $^{16}O(p,p)^{16}O$ elastic scattering cross section at $\vartheta_{c.m.}=171.5°$ in the energy region below 2.0 MeV (solid curve) with experimental data from Ref.[15]. Ref.[6] prediction of the proton energy at which the scattering cross section deviates by 4% from its Rutherford value is shown by dashed lines.

3.2. Resonance scattering.

Resonance scattering was taken into account using S-matrix theory in the way L.Veeser and W.Haeberli [17] did. The differential cross section can be written in terms of amplitudes $f_l^{\pm}$ which are related to the S-matrix elements by

$$f_l^{\pm} = (S_l^{\pm} - 1) / 2i$$

The diagonal elements of the scattering matrix were assumed to be of the form

$$S_l^{\pm} = exp(2i\lambda_l^{\pm})\left[exp(-2\mu_l^{\pm}) + exp(2i\phi_p)\frac{i\Gamma_p}{E_0 - E - \frac{1}{2}i\Gamma_p}\right],$$

where $\lambda_l^{\pm} + \mu_l^{\pm}$ is the off-resonance nuclear phase shift describing the elastic scattering of protons of energy E from spin zero nuclei. The quantities E_0, Γ and Γ_p are the energy, total width and partial elastic width, respectively. The subscript l is the relative angular momentum of the proton and the target in units of $\hbar$. The plus sign refers to the case when $J=l+1/2$ and the minus sign to the case when $J=l-1/2$. The quantity ϕ_p is a resonance phase shift. The off-resonance scattering matrix elements were calculated in the framework of the optical model. A computer program SCAT2 [12] has been modificated to calculate the differential cross section according to the above equations. Application of the described theory to cross section representation is demonstrated in section 4.1.

3.3. Deuteron induced reactions.

At the first stage of a theoretical description of the (d, p)- reaction at low deuteron energies it was assumed that the main contribution to the cross section of the process is given by the following three mechanisms: direct stripping, resonant mechanism and in some cases a compound nucleus mechanism. While evaluation of a role of resonant scattering it was assumed, that the complete amplitude T of process is $T=D+R$, where D is the amplitude of the direct process of stripping, which was calculated within the framework of a method of deformed waves without the account of effects of a recoil nucleus, and R-is the amplitude of resonant process,

calculated in frameworks of a single level approximation. Complete and partial width of formation and disintegration of resonances in the system, which are necessary in order to calculate the amplitude of R, were defined by fitting the model predictions to the available experimental cross sections of elastic deuteron scattering and (d, p)-reaction.

Before search of free parameters of the model the contribution of the compound scattering was evaluated and the experimental (d, p)- reaction cross sections were appropriately modified. The satisfactory description of the experimental data by the theoretical model is as a whole observed (see Fig.4). However, for a reliable description of a whole set of (d,p)-reaction data a development of the model in several directions is required.

First, it is necessary more strictly to determine a role of a compound nucleus mechanism in (d,p)-reaction in a wide kinematics range. In calculations performed within the framework of Hauser-Feshbach-Moldauer model [18] the contribution of the compound mechanism at backward scattering angles is about of 50 % of total cross section. However, as appear, the contribution of this mechanism is essentially overestimated for the several reasons: (i) owing to low binding energy of a deuteron and its electric charge distribution asymmetry; (ii) due to the fact that since light nuclei have low number of particles and the quantum mechanics forbidden rules are strong for these nuclei they have low internal degrees of freedom and consequently the equilibrium processes in the particle system of this type are essentially suppressed.

Secondly, there are problems in the description of a direct component of an interaction. For the DWBA calculations of reactions with light fragments it is necessary to take into account a final radius of interaction and the effects of a multiple projectile-target exchange of nucleons.

Thirdly, at a collision of deuterons with nuclei in addition to the compound nucleus mechanism and the direct (d,p) stripping reactions also direct exchange processes of knock-out and heavy stripping are possible.

In - fourth, it is necessary correctly to evaluate a role of a resonant mechanism in case of strongly overlapped resonances. The problem of taking into account the close lying resonances interference is far beyond the limits of the simplified approach of single level approximation employed in the performed calculations. Actually the interaction of disintegrating states should be taken into account. To choose that or other physical concept for the analysis of the area of a spectrum, where the levels are strongly overlapped, it is necessary to resolve a number of important problems, requiring further research.

The equations used and a detailed description of the calculations briefly outlined above will be published [19].

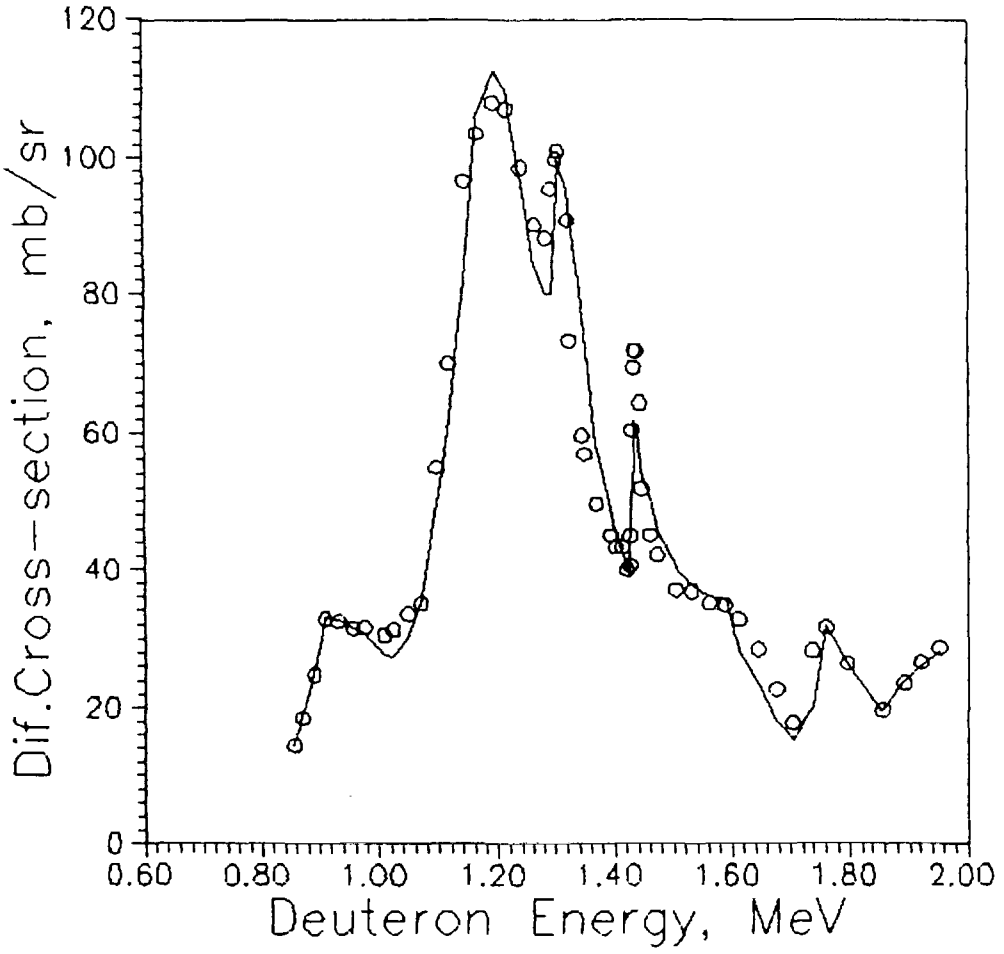

Fig.4. The results of $^{12}C(d,p_0)$-reaction cross section calculations. Circles - experimental data measured at 165°[20], with compound nucleus mechanism contribution being subtracted. Solid line - theoretical calculations as described in the text.

4. Measurements.

4.1. Elastic $^{16}O(p,p)^{16}O$ scattering.

Measurements of the differential $^{16}O(p,p)^{16}O$ elastic scattering cross sections were performed using a proton beam from IPPE tandem generator in the energy range from 3.2 to 4.2 MeV at laboratories angles 125°, 145°, and 165°. The accelerator energy was calibrated using a nuclear resonance in the $^{12}C(p,p_0)^{12}C$ elastic scattering at E_p=4.806 MeV ("secondary" point). A self-supporting film of Al_2O_3 about 60 μg/cm^2 thick was used as a target. Calculations show that neither inelastically scattered from ^{27}Al protons nor particles from nuclear reactions interfere with protons elastically scattered from ^{16}O in the energy range under investigation. A thin gold

layer was deposited on the film by vacuum evaporation to provide electric conductivity of the target. As far as elastic scattering from gold in the employed energy range is pure Rutherford one, it was used also as internal standard. Absolute values of the cross sections were obtained by performing the measurement at 3.1 MeV at 170° and assuming the cross section to be equal to its value from Ref.[14]. Relative experimental errors were estimated to be about 3%.

Two strong resonances are observed in the studied energy range [21]. The $F_{7/2}$ resonance width at 3.47 MeV is reported to be 1.53 keV that is less than used energy beam resolution, while the $D_{3/2}$ resonance at 4.26 MeV is very broad (about 220 keV). Consequently the last one influenced the cross section in a wide energy range. Experimental results for θ_{lab}=165° along with theoretical curve calculated by the method described in section 3.2 are presented in Fig.5.

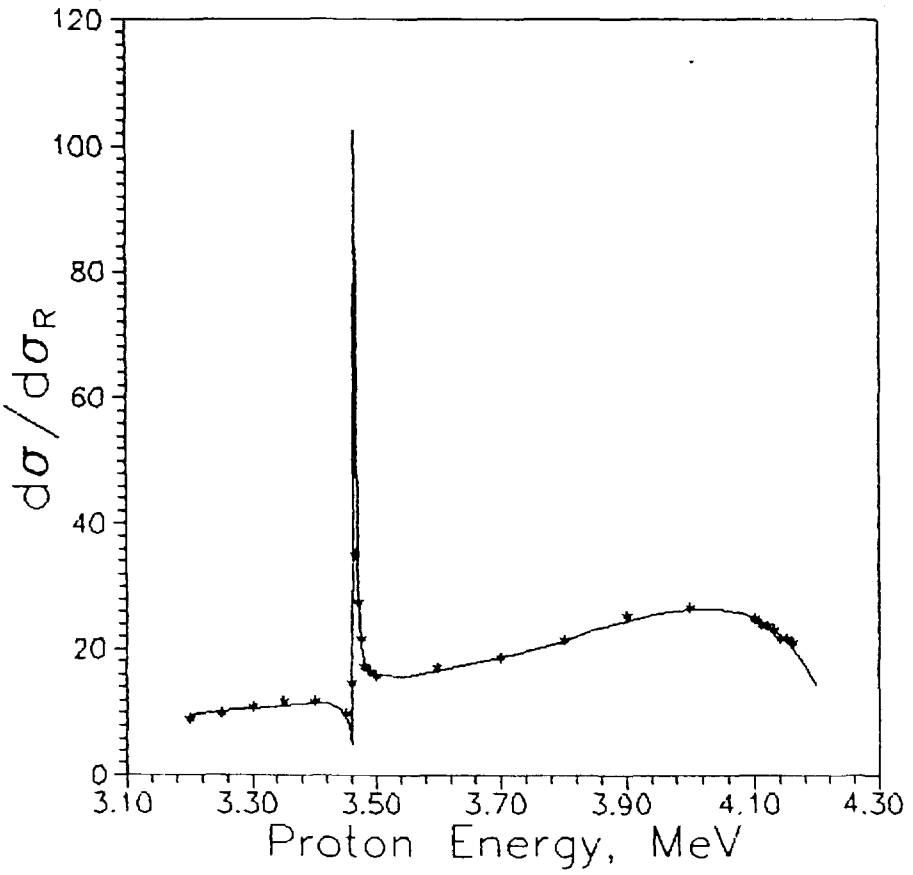

Fig.5. Measured elastic $^{16}O(p,p)^{16}O$ cross section at θ_{lab}=165° and its theoretical representation. Resonances at E_p=3.470 MeV and E_p=4.260 MeV are taken into account as described in Section 3.2.

4.2. Elastic $^{56}Fe(p,p)^{56}Fe$ scattering.

Differential cross sections of proton elastic scattering from ^{56}Fe was measured in the energy interval from 3.7 to 4.3 MeV. The cross section has resonance like structure in this energy region caused by isobaric analog resonances and by Ericson fluctuations. The measurements of these cross sections have been reported [22] but their rather complicated structure prevents from reliable application of digitizing procedure. The utility of the relatively high energy proton backscattering for investigation of thick metal films was demonstrated in Ref.[23].

The measurements were made at EGP-10M tandem generator by 5 keV steps using 0.23 mg/cm^2 thick self-supporting enriched ^{56}Fe target. The target thickness and homogeneity were determined in the low energy ^4He backscattering experiment using EG-2.5 Van de Graaff accelerator. Charge collection was used to obtain absolute cross section values. The results are presented in Fig.6.

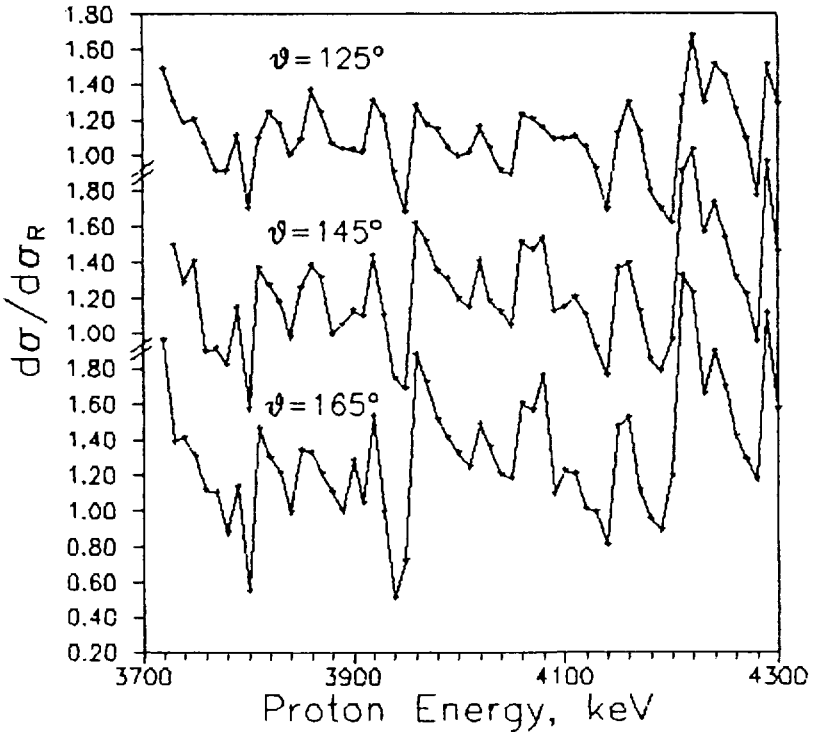

Fig.6. Differential $^{56}Fe(p,p)^{56}Fe$ proton elastic scattering cross sections. Every second point has been plotted. Lines were drawn to guide an eye.

4.3. Resonance $^{23}Na(p,p'\gamma)^{23}Na$ reaction.

Thick target excitation yield of prompt gamma-rays are often measured and published as graphs and tables. In the case of narrow resonances used in resonance depth profiling, an yield

curve seems to be not the best way to represent the cross section, which can only be expressed mathematically in the vicinity of a narrow resonance.

Resonance yield per unity solid angle and incident particles charge for prompt gamma-rays emission from homogenous target with energy thickness of ΔE_T is defined as

$$Y = c\frac{N_0}{A}\int_{E-\Delta E_T}^{E}\frac{\sigma(p,\gamma)}{dE/dx}dE, \qquad (2.1)$$

where N_0 - is Avogadro constant, A - is a molecular mass, c - is element concentration in the target.

Assuming a Breit-Wigner resonance

$$\sigma(p,\gamma) = \sigma_R\frac{\Gamma^2/4}{(E-E_R)^2+\frac{\Gamma^2}{4}}, \qquad (2.2)$$

where σ_R - is a cross section at resonance energy E_R and Γ - is a resonance width,

the yield for an infinitely thick target ($\Delta E_T >> \Gamma$) is

$$Y = \frac{cN_0}{2A}\frac{\sigma_R\Gamma}{dE/dx}\left(\frac{\pi}{2}+tan^{-1}\frac{E-E_R}{\Gamma/2}\right). \qquad (2.3)$$

The σ_R, Γ, and E_R may be regarded as free parameters and these have to be found by fit of theoretical yield defined by eq.(2.3) to measured data.

The mathematics outlined above was applied for the case of $^{23}Na(p,p_1\gamma)^{23}Na$ reaction. The resonance located at $E_R \cong 1457$ keV which has strengths defined by $S=(2J+1)\Gamma_p\Gamma_{p\gamma}/\Gamma$ as great as 1700 eV [24] has been chosen as most suitable for resonance depth profiling due to it strength, relative narrowness and because of sufficiently wide energy gap separated this resonance from both sides. A measurement of the 439 keV gamma-rays was made in the vicinity of the resonance using a thick NaCl target which was bombarded with proton beam from the EG-2.5 Van de Graaff accelerator of IPPE. The emitted γ-radiation was detected by a Ge(Li) detector at an angle of 90° with respect to the incident proton beam. Absolute data were obtained by calibration of detection efficiency using standard γ-rays sources placed in the scattering chamber in the position of beam spot on the target and by collection of incident protons charge. The accelerator was calibrated using 991.9 keV resonance in $^{27}Al(p,\gamma)^{28}Si$ reaction. Intensity of chlorine gamma-rays is very low and this radiation does not interfere with sodium emission. The results of the measurement and a theoretical description of γ-emission yield are presented in Fig.7. Data from Ref.[25] are also shown in the Fig.7 for comparison.

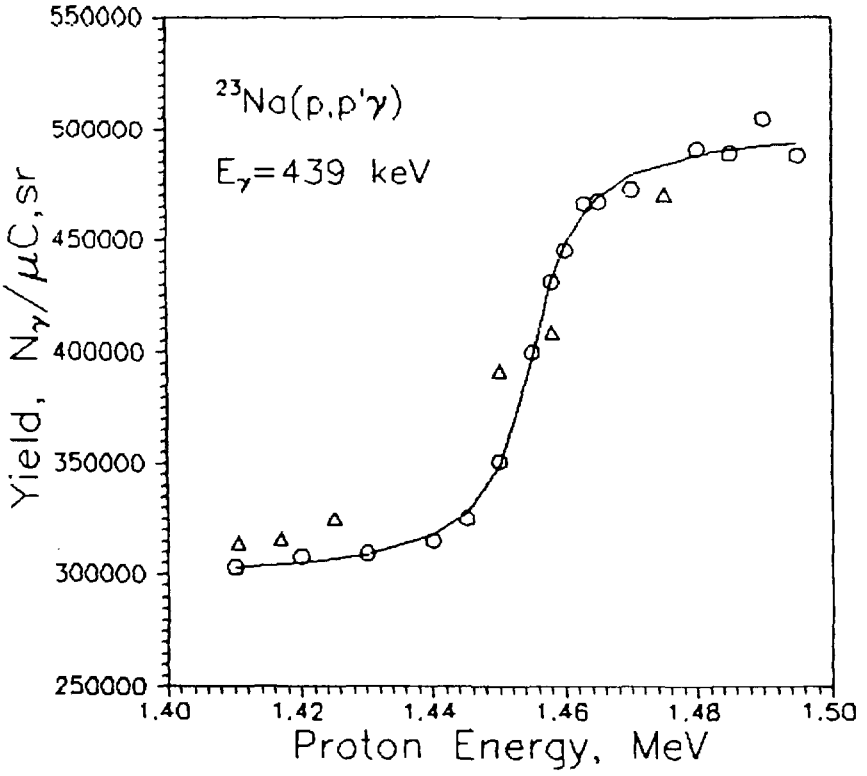

Fig.7. Thick target excitation curve for the ^{23}Na(p,p'γ)^{23}Na reaction (E_γ=439 keV) in the vicinity of the resonance (circles) and its theoretical description (solid line). Data from Ref.[25] are shown by triangles.

Deduced resonance parameters E_R=1456±1.8 keV and Γ=8.3±0.8 keV, the last quantity being corrected for instrumental width, appears to be in a close agreement with Ref.[24].

5. Results.

Compilation of the cross sections data resulted in producing a new version of the NRABASE data base. New digitizing procedure was used and some technical improvements in data organization and presenetation were made. The NRABASE description was published as a paper [5].

Theoretical model approach to Non-Rutherford elastic scattering cross section evaluation has been developed. Its utility has been demonstrated. The same was made for resonance reactions. Theoretical model approach for deutron induced reactions reveals some problems which are under investigation.

Measurements of the differential cross sections for the ^{16}O(p,p)^{16}O elastic non-Rutherford scattering in the energy range 3.2 - 4.2 MeV have been performed. The same has been made for

$^{56}Fe(p,p)^{56}Fe$ in energy range 3.7 - 4.3 MeV. Thick target excitation yield of prompt gamma-rays was measured for $^{23}Na(p,p'\gamma)^{23}Na$ reaction in the vicinity of strong resonance at E_p=1457 keV.

References

1. I.C.Vickridge, Nucl. Instr. and. Meth. B66 (1992) 303.
2. J.P.F.Sellschop and S.H.Connel, Nucl. Instr. and. Meth. B85 (1994) 1.
3. J.M.Knox and J.F.Harmon, Nucl. Instr. and Meth, B44 (1989) 40
4. Handbook of Modern Ion Beam Materials Analysis, Ed. J.R.Tesmer and M.Nastasi, MRS, Pittsburg, 1995, p.481.
5. А.Ф.Гурбич, В.А.Ершова, Вопросы Атомной Науки и Техники, Сер.: Ядерные константы, вып. 1, 1996, с.99.
6. M.Bozoian et al., Nucl. Instr. and Meth. B51 (1990) 311; B56/57 (1991) 740; B58 (1991) 121, B58 (1991) 127, B82 (1993) 602.
7. J.Tang, Y.Sun, H.Cheng, H.Shen, Nucl. Instr. and Meth. B74 (1993) 491.
8. 8.F.G.Perey, Phys. Rev. v.131 (1963) p.745.
9. F.D.Bechetti, G.W.Greenlees, Phys. Rev. v.182 (1969) p.1190.
10. S.Kailas et al. Phys. Rev. v.C20 (1979) p.1272.
11. А.Ф.Гурбич, Диссертация, Киев, 1983.
12. O.Bersillon, Centre d'Etudes de Bruyeres-le-Chatel Note CEA-N-2227, 1981.
13. I.Ahmad, W.Haider, J.Phys. v.G2 (1976) p.L157.
14. Yang Guohua et al. Nucl. Instr. and Meth. B61 (1991) 175.
15. H.C.Chow, G.M.Griffiths, T.H.Hall, Can. J. Phys. v.53 (1975) p.1672.
16. M.Luomajarvi, E.Rauhala, M.Hautala, Nucl. Instr. and Meth. B9 (1985) 255.
17. L.Veeser, W.Haeberli, Nucl. Phys. v.A115 (1968) p.172.
18. W.Hauser, H.Feshbach, Phys.Rev. v.87 (1952) p.366; P.A.Moldauer, Rev.Mod.Phys. v.36 (1964) p.1079.
19. Н.Н.Титаренко, Препринт ФЭИ, to be published.
20. E.Kashy, R.R.Perry, J.R.Risser, Phys. Rev. v.117 (1966) p.1289.
21. R.A.Laubenstein, M.J.W.Laubenstein, L.J.Koester, R.C.Mobley, Phys. Rev. v.84 (1951) p.12.
22. H.Brandle, W.R.Wylie, F.Zamboni, W.Zych, Nucl. Phys. v.A151 (1970) p.211.
23. Е.А.Романовский и др., Поверхность. N^0 8-9 (1994) 123.
24. M.A.Meyer, J.P.L.Reinecke, D.Reitmann, Nucl. Phys. v.A185 (1972) p.625.
25. F.Bodart, G.Deconninck, G.Demortier, J. Rad. Chem. v.35 (1977) p.95.